THE JOURNAL OF PHYSICAL CHEMISTRY B
A JOURNAL OF THE AMERICAN CHEMICAL SOCIETY

pubs.acs.org/JPCB

Article

Crystal Growth Kinetics in GeS_2 Glass and Viscosity of Supercooled Liquid

Jiří Málek,* Veronika Podzemná, and Jana Shánělová

Cite This: https://doi.org/10.1021/acs.jpcb.1c03243

Read Online

ACCESS | Metrics & More | Article Recommendations

ABSTRACT: The crystal growth kinetics and morphology in germanium disulfide bulk glass and glass surface is described. The structural relaxation taking place below the glass transition is slow and the corresponding volumetric change is negligible. Therefore, it does not affect substantially the crystal growth process. The crystal growth rate of low temperature β-GeS_2 and high temperature α-GeS_2 polymorphs in the bulk glass is comparable, being slightly decoupled from the shear viscosity below the glass transition. The crystal growth rate of β-GeS_2 in an amorphous thin film of the same composition is several orders of magnitude faster than that at the surface of bulk glass. This fast surface crystal growth is strongly decoupled from viscosity. Such behavior resembles the glass-to-crystal fast growth mode observed by several authors in some organic molecular glasses. Taking into account previously reported viscosity and heat capacity data, the crystal growth kinetics of both polymorphs can be quantitatively described by the 2D surface growth model for low and high supercooling. The nonisothermal differential scanning calorimetry experiments are analyzed, providing evidence of a complex nature of the overall crystallization process with apparent activation energy comparable to that obtained from isothermal microscopy measurement of crystal growth in the same temperature range.

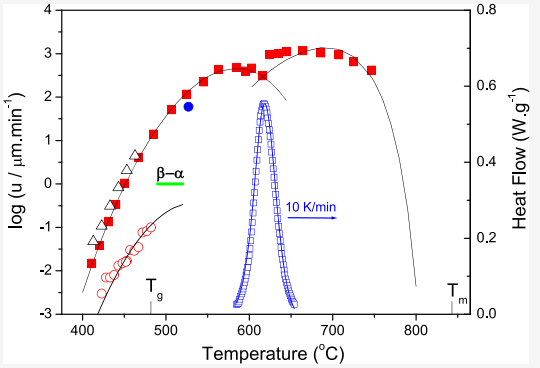

1. INTRODUCTION

Materials with a layered crystal structure and high in-plane anisotropy are promising for applications in photonic and electronic devices. Two-dimensional germanium disulfide exhibiting high in-plane anisotropy and a wide band gap was recently used as a polarization-sensitive photodetector in the ultraviolet spectral region.[1] The origin of this anisotropy has been analyzed and explained by ordered and disordered arrangement of corner-shared GeS_4 tetrahedra in the GeS_2 monolayer.[2]

The crystal structure of a high temperature polymorph (α-GeS_2) was determined by Dittmar and Schäffer[3] as a two-dimensional (2D) network layer assembly. A single layer is formed by chains of corner-linked GeS_4 tetrahedra, cross-linked by edge-sharing tetrahedra, running parallel to the *a*-axis. This means that there are pairs of Ge atoms, which are connected by two sulfur bridges, producing six and four member rings in a 2:1 ratio. The structure crystallizes in the monoclinic space group $P2_1/c$.[3] The energy of exfoliation calculated by Wang et al.[2] is 11 meV/Å, being about one half of that of MoS_2.[2] In contrast, the low temperature polymorph (β-GeS_2) has a more complicated three-dimensional (3D) structure containing large elliptical hollows surrounded by 24 corner-sharing GeS_4 tetrahedra, together with six-member rings. It crystallizes in the monoclinic space group *Pc*.[4,5] This β polymorph was found to be stable with excess sulfur below 497 °C and in equilibrium with germanium monosulfide below 520 °C.[6] The transition rate between high and low temperature polymorphs is very slow. The β-GeS_2 nanoplates prepared by a low temperature solvothermal process exhibit considerable photocatalytic activity for hydrogen generation from light-driven water splitting.[7]

The structure of germanium disulfide glass has been investigated by various experimental methods[8−10] and also by molecular dynamics simulations.[11,12] Usually it is assumed that the network structure of this glass is formed by the connection of edge-sharing and corner-sharing GeS_4 tetrahedra. Nevertheless, it is uneasy to determine whether the structure of GeS_2 glass is similar to the 2D-layered α-GeS_2 or 3D network β-GeS_2 polymorph. Phillips[13] argued that the structural difference between α-GeS_2 and β-GeS_2 is actually subtle as there are only chalcogen atoms at the internal surfaces (layers or hollows). The topological difference then stems from the radius of curvature of these internal surfaces,

Received: April 10, 2021
Revised: May 31, 2021

which is infinite (layers) for α-GeS_2 but finite (hollows) for β-GeS_2. Weinstein et al.[14] carried out nice experiments to determine the effect of pressure on the optical absorption edge and near-infrared refractive index of both crystalline forms and GeS_2 glass. Their analysis has clearly shown that GeS_2 glass is not a 3D network similar to SiO_2 but instead has a lower network dimensionality typical for molecular glasses. In this particular case the observed behavior was not so different from α-GeS_2. It seems, therefore, that the medium range order of the germanium sulfide glass is probably similar to that of the crystalline polymorph α-GeS_2, although the dimensionality of the network is higher than 2D and of course there is no long-range order. A similar conclusion was also suggested by other authors on the basis of spectroscopic[15,16] and calorimetric[17] experiments. In contrast, Černošek et al.[18] reported that the medium range structure of GeS_2 glass is similar to that of the 3D network of β-GeS_2. Recently, Itoh[19] used pulsed neutron diffraction and reverse Monte Carlo modeling methods to study the structure of GeS_2 glass. This analysis revealed that both the 2D layer network and 3D random network are plausible theoretical description reproducing experimental data of glassy germanium disulfide. The structural changes below the glass transition temperature (T_g) are effectively hindered as the displacement of larger structural units becomes difficult due to the cooperative nature of structural relaxation. It can be expected that crystalline phases grown under these conditions should reflect the structural similarities with the glassy state.

The aim of this paper is to provide a detailed study of crystal growth behavior of stoichiometric GeS_2 glass below and above the glass transition. A significant difference between bulk, surface, and thin film growth is discussed and compared to the fast glass-to-crystal growth mode observed in organic molecular glasses, addressing still the open question of germanium disulfide network dimensionality in a glassy state as well as the effect of structural relaxation. The crystal growth velocity is combined with thermodynamic and viscosity data and described by a 2D surface growth model. The microscopic crystal growth velocities are compared with macroscopic calorimetric experiments that are typically used for crystal growth studies in glassy materials.

2. MATERIALS AND METHODS

The GeS_2 glass was prepared from standard high purity (5 N) elements (sulfur was additionally purified by multiple distillation). Stoichiometric amounts of these elements (8 g total weight) were placed into a carefully washed and dried silica glass ampoule (16 mm inner diameter, 1 mm wall thickness, and 80 mm length). The ampoule was then evacuated to a pressure of 10^{-3} Pa for 1 h and then sealed. The sealed ampoule was then placed in a rocking furnace and held at 430 °C for 4 h to provide a better reaction between Ge and S and then homogenized and melted completely at 950 °C for 24 h. The GeS_2 glass bulk was then prepared by a rapid quench of the ampoule in ice water. For this setup we can expect a cooling rate of about 600 K/min.[20] Then, the ampoule was opened and the as-prepared GeS_2 glassy ingot of light-yellow color and a typical conchoidal fracture was sectioned by a diamond saw to small specimens (approx. 1 mm thickness). These specimens were polished by a standard technique to optical quality and then stored for subsequent treatment in a desiccator. About 10 different batches of germanium disulfide glass were prepared and analyzed during several years to verify reproducibility of crystal growth measurements.

The isothermal crystal growth kinetics was studied by an Olympus BX51 optical microscope equipped with a DP72 digital camera. All samples were optically transparent, and therefore, the crystal growth measurements could be performed in a transmission mode (the optical gap for GeS_2 glass and crystal is higher than 3 eV). The sizable difference in reflectivity between the amorphous glass and crystalline phase enables observation and measurement of crystal growth. Direct measurement in a real time is not suitable as it does not allow a careful and detailed observation of distinct phases of development of growing crystal facets. For this reason, all samples were previously heat-treated in a computer-controlled furnace for various time spans at preselected temperatures. A complete thermal history of the samples was recorded (central hot zone was constant within ±0.5 K). The selected temperature range for the bulk and thin film samples represents an optimum choice because outside of the range the crystal growth rate is either too high or too slow to be observed by this microscopy technique.

The nonisothermal crystal growth kinetics was studied by differential thermal analysis (PerkinElmer DTA-1700/TADS) in a heat-flux differential scanning calorimetry (DSC) mode. Due to high volatility of germanium disulfide at elevated temperature, all measurements were carried out using a small amount of germanium disulfide (20 mg) placed in a small evacuated silica ampoule fitting a platinum sample holder. Dry alumina powder placed in the same container was used as the reference sample. The instrument was calibrated using pure metal standards (In, Sn, Pb, Al, Ag, and Au). The thermal expansion measurement was measured by a thermomechanical analyzer (R.M.I., TMA CX 02R) equipped with a capacitance displacement detector (low noise, 0.01 μm resolution, ±0.2 K temperature stability). To avoid penetration of the probe into the specimen above T_g, the measurements were performed using a sample inserted between two polished quartz plates of 5 × 5 mm. A low scanning rate was used (±3 K/min) and the specimen was loaded by a force of 10 mN.

The composition of the prepared materials and crystalline phases grown during the thermal treatment was confirmed by an energy dispersive X-ray (EDX) microanalyzer IXRF Systems (detector GRESHAM Sirius 10) coupled with a scanning electron microscope (JEOL JSM-7500 F). The amorphous nature of the as-prepared samples and crystalline structures was verified by using X-ray diffraction analysis (Bruker AXS diffractometer D8 Advance, Cu Kα 40 kV, 30 mA).

3. RESULTS

The crystal growth process in GeS_2 bulk glass starts at temperatures well below the T_g from randomly distributed nuclei. Two different types of crystal morphology were observed. Characteristic compact spherulitic structures are growing in the bulk and at the sample surface.

Figure 1a shows α-GeS_2 spherulite grown in the germanium disulfide bulk glass at higher temperature. White crystals of β-GeS_2 visible in the central and external part of spherulites are formed after subsequent annealing below T_g. Figure1b shows typical β-GeS_2 spherulites formed at the bulk glass surface. Small preexisting crystals of α-GeS_2 dispersed in some cases in the glassy bulk matrix grow to characteristic thin hexagonal plates at short annealing times below T_g (Figure 1c). More

https://doi.org/10.1021/acs.jpcb.1c03243
J. Phys. Chem. B XXXX, XXX, XXX−XXX

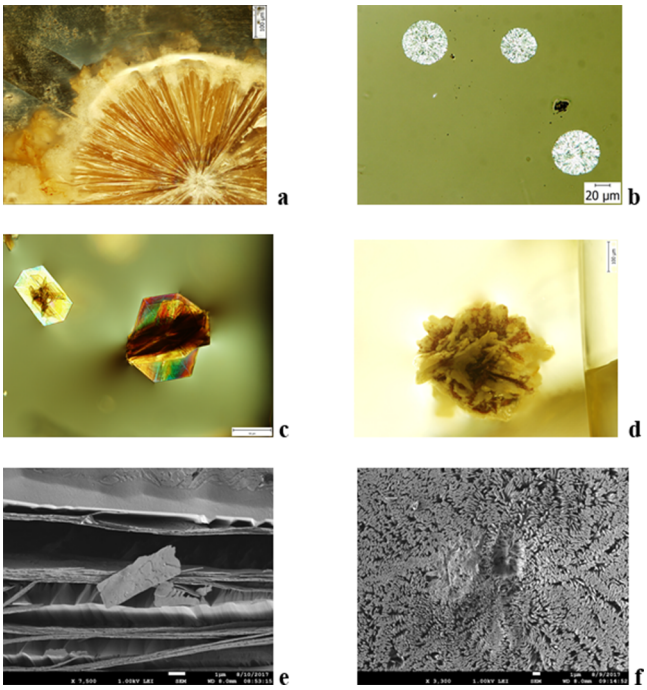

Figure 1. Morphology of GeS_2 crystals. Optical microscopy, polarized light: (a) α-GeS_2 spherulite grown in the bulk at higher temperature (orange color); (b) β-GeS_2 spherulites grown at the surface at lower temperatures; (c) α-GeS_2 grown in the bulk; and (d) β-GeS_2 grown in the bulk. SEM, the specimen surface after longer annealing times, etched in alkaline solution: (e) exfoliating layers of α-GeS_2 and (f) spherulitic surface of β-GeS_2.

complex aggregate crystalline structures of β-GeS_2 are formed at longer annealing times (Figure 1d). Figure 1e displays the SEM photograph of α-GeS_2 showing weakly coupled layers in a vertical direction, in contrast to a compact structure along planar directions. These layers can easily be exfoliated from the bulk structure.[2] A quite different picture is seen for β-GeS_2. In this case, the compact spherulitic structures are formed below T_g. Figure 1f shows the SEM image of the spherulitic surface with clearly visible spatial distribution of thin crystalline needles composing a dense spherulite of β-GeS_2.

The EDX microanalysis on partially crystalline and etched specimens confirmed that both type of crystals corresponds to GeS_2 composition. Platelike crystallites showing characteristic habitus defined by lateral planes (0 0 1), (0 0 1−) and head planes (3 4 0), (3 2− 0) correspond to the high temperature α-GeS_2 (Figure 1c).[3] The compact spherulitic aggregates were identified as low temperature β-GeS_2 (Figure 1b) and high temperature α-GeS_2 (Figure 1a). They are composed of fine needles or lamellae radiating from a spherulitic center and clearly visible in polarized light.

The specimens of germanium disulfide glass polished to optical quality were isothermally annealed for a defined period of time at selected temperatures in a precisely controlled preheated furnace. Then, the specimens were rapidly quenched to room temperature and dominant crystal size of isolated crystals, crystalline aggregates, or spherulitic diameters were measured repeatedly for about 10 independent and separate objects. The crystals were mostly grown from preexisting nuclei, randomly distributed within the specimen. It was confirmed that the crystal size is linearly dependent on time at all temperatures selected. This is a typical behavior for crystal growth controlled by kinetics at a crystal−amorphous phase interface. The crystal growth velocity u was determined as the slope of these linear dependences. The time scale for microscopy observation was about 3−5 min for highest temperatures and 10−60 h for lowest temperatures. Experimental crystal growth velocity data for spherulitic crystal growth rate at the surface of GeS_2 glass are summarized in Table 1. The experimental data for crystal growth in the GeS_2 bulk glass are shown in Table 2.

Table 1. Crystal Growth Velocity of β-GeS_2 at the Glassy Surface

T (°C)	u (μm·min^{-1})
411.1	0.003 ± 0.001
423.0	0.003 ± 0.001
428.0	0.007 ± 0.001
431.0	0.005 ± 0.001
433.0	0.007 ± 0.001
438.0	0.008 ± 0.002
443.0	0.013 ± 0.003
448.0	0.015 ± 0.007
453.0	0.017 ± 0.005
452.2	0.016 ± 0.005
457.1	0.030 ± 0.006
461.9	0.029 ± 0.005
466.8	0.035 ± 0.009
471.7	0.076 ± 0.009
476.5	0.082 ± 0.019
481.4	0.10 ± 0.018

It is known that the germanium disulfide glass supercooled melt is vulnerable to crystallization, and in fact, it is not so easy to prepare a stoichiometric GeS_2 free from crystalline inclusions.[21] A typical crystalline phase present in some specimens is a high temperature α-GeS_2 polymorph in the

Table 2. Crystal Growth Velocity in the Bulk Glass

T (°C)	u (μm·min^{-1})	
411.1	0.015 ± 0.004	... β-GeS_2
420.3	0.038 ± 0.008	
431.0	0.133 ± 0.015	
439.9	0.338 ± 0.045	
450.7	1.04 ± 0.31	
467.3	4.10 ± 0.51	
485.1	14.02 ± 0.95	... β-GeS_2 + α-GeS_2
506.7	50.70 ± 4.30	
525.0	117 ± 14	... α-GeS_2
445.4	223 ± 24	
563.1	430 ± 37	
584.5	479 ± 154	
595.6	395 ± 63	
602.9	464 ± 158	
616.2	307 ± 71	
624.7	952 ± 102	
634.7	993 ± 79	
644.3	1103 ± 165	
664.4	1164 ± 259	
685.8	1031 ± 216	
707.3	934 ± 175	
725.0	643 ± 90	
746.5	420 ± 72	

https://doi.org/10.1021/acs.jpcb.1c03243
J. Phys. Chem. B XXXX, XXX, XXX−XXX

form of thin plates of hexagonal habitus. These crystals are grown upon heating. Their crystal growth velocities at different temperatures are summarized in Table 3.

Table 3. Crystal Growth Velocity of Preexisting α-GeS_2 in the Bulk Glass

T (°C)	u (μm·min^{-1})
413.0	0.047 ± 0.011
423.0	0.107 ± 0.023
433.0	0.308 ± 0.082
443.0	0.82 ± 0.16
453.0	2.05 ± 0.34
463.0	4.41 ± 1.18

Temperature-dependent crystal growth velocities at the surface and in the bulk of germanium disulfide glass are compared in Figure 2 on a logarithmic scale. Further crystal

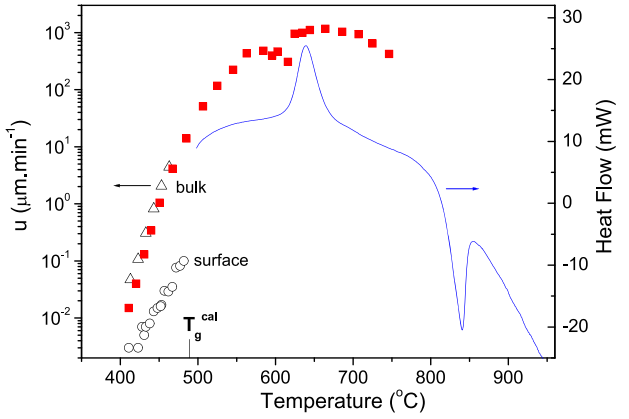

Figure 2. DSC curve (20 K/min) of GeS_2 glass (solid line). The temperature dependence of the isothermal crystal growth velocity of α-GeS_2 (triangle), β-GeS_2 + α-GeS_2 (solid square) in the bulk glass, and β-GeS_2 at the bulk surface (circle).

growth of preexisting α-GeS_2 crystals takes place simultaneously with a surface growth of spherulitic β-GeS_2 at temperatures well below T_g. Similar behavior was observed earlier for $Ge_{0.38}S_{0.62}$ glass, where the growth velocities of both GeS_2 polymorphs are also comparable, though taking place above the glass transition.[22] It is clearly seen that crystals in the bulk of germanium disulfide glass grow significantly faster than spherulites at the surface ($u_b/u_s \cong 70$).

The heat flow evolved during the crystallization process can easily be detected by a sensitive instrument operating in the DSC mode. Figure 2 shows DSC data (20 K/min) measured from the calorimetric glass transition (T_g^{cal} = 489 °C)[23] to temperatures well above the melting point. The enthalpy change of the crystallization process ΔH_c can be obtained by integration of the measured heat flow over the whole crystallization peak. For DSC data shown in Figure 2, it was found to be $\Delta H_c = -102 \pm 12$ J/g. The standard mass enthalpy of the transition of GeS_2 from the glassy to crystalline state, determined by O'Hare et al.[24] by fluorine combustion calorimetry ($\Delta_{trs}H° = -91.3 \pm 10.8$ J/g) is lower, but still in a relatively good agreement taking into account quite different calorimetric techniques used for measurement.

Figure 3 shows the thermal contraction of GeS_2 supercooled liquid measured by thermomechanical analysis during slow

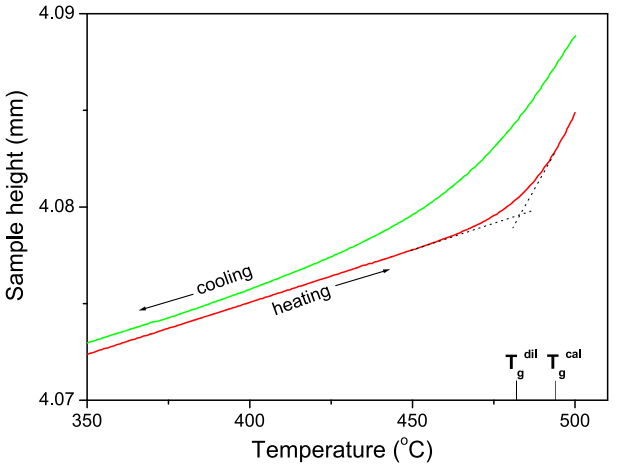

Figure 3. Dilatometric data for cooling (−3 K/min) and subsequent heating (+3 K/min) of GeS_2 glass (applied force: 10 mN).

cooling (−3 K/min) from temperature 500 °C where a metastable equilibrium is attained for a short time, unless the crystallization starts. The glass "quenched" at this slow cooling rate is subsequently reheated (+3 K/min) to the same temperature. The dilatometric glass transition (T_g^{dil} = 482 °C) is defined as the intersection of a line representing the thermal expansion coefficient of the glassy state on heating $\alpha_g = (dl/dT)/l_o = 12 \times 10^{-6}$ K^{-1} and that of supercooled liquid ($\alpha_l \cong 72 \times 10^{-6}$ K^{-1}). As expected, the dilatometric glass transition is 7 K lower than T_g^{cal}, due to different experimental timescales (t_{exp}), as well as different ways of determination. A slight difference in the sample height (≈ 0.6 μm) observed below 400 °C is caused by sample deformation due to nonlinear structural relaxation[25] and viscous flow during cooling in the glass transition range.

4. DISCUSSION

4.1. Viscosity and Structural Relaxation. For moderate stress, the supercooled liquid above the glass transition has the rheological properties of a linear viscoelastic medium. In this case we can use the simplified Maxwell model based on the assumption that shear flow is the superposition of viscous and elastic contribution.[26] The single shear relaxation time τ_R is then approximately related to shear viscosity η by

$$\tau_R = \eta / G_\infty \quad (1)$$

where G_∞ is the infinite frequency shear modulus. The temperature dependence of shear viscosity of a glass-forming supercooled liquid can be expressed in the form of MYEGA equation:[27]

$$\log \eta = \log \eta_0 + (12 - \log \eta_0) \times \left(\frac{T_{12}}{T}\right) \exp\left[\left(\frac{m}{12 - \log \eta_0} - 1\right) \times \left(\frac{T_{12}}{T} - 1\right)\right] \quad (2)$$

where η_0 is the extrapolated infinite temperature viscosity, T_{12} is the "*viscosity glass transition*" (i.e., temperature where the shear viscosity is equal to 10^{12} Pa s) and m is fragility at T_{12}. Taking into account the reported viscosity data for the GeS_2 melt[28] we can calculate: $\log(\eta_0/\text{Pa s}) = -5$, T_{12} = 726.4 ± 0.9 K, and m = 35.32 ± 1.10. Ota and Kunugi[29] reported the value of shear modulus G_∞ = 6.06 GPa. From eqs 1 and 2, we can

https://doi.org/10.1021/acs.jpcb.1c03243
J. Phys. Chem. B XXXX, XXX, XXX−XXX

estimate the relaxation time at the dilatometric glass transition (T_g^{dil}) as $\tau_R \approx 8$ s.

As a supercooled liquid is cooled to lower temperatures, its viscosity rapidly increases and molecular movement gradually slows down in such a way that for the liquid, it becomes difficult to attain metastable equilibrium.[26] We can define the glass transition as the temperature T_g where the time scale for molecular rearrangements τ approaches the experimental time scale ($\tau \approx t_{exp}$).[30] Therefore, the temperature where the glass transition occurs depends on the actual value of t_{exp}, i.e., on the cooling rate. The glassy state below T_g^{dil} is out of equilibrium with broken ergodicity. It has important consequences. At $T < T_g^{dil}$ the glass structurally relaxes toward the metastable equilibrium state extrapolated from supercooled liquid.[25] The GeS_2 glass below T_g^{dil} exhibits the heat capacity and thermal expansion coefficient typical for a solid material. However, the structural relaxation takes place even 60 K below T_g^{dil}, though its rate is extremely slow. In fact, the structural relaxation can be considered as a subtle and more complex continuation of viscous flow.[31]

These features can easily be shown by a simple experiment: the cooling during the dilatometric measurement (see Figure 3) is halted at 462 °C ($l = l_0$) and then the sample length is recorded as a function of time. Figure 4 shows a plot of relative

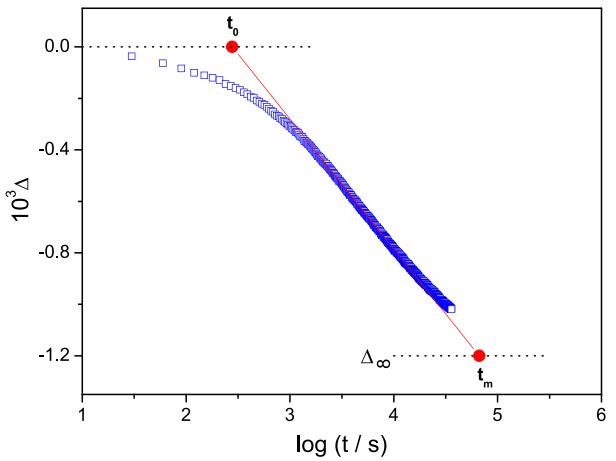

Figure 4. Isothermal length contraction $\Delta = (l - l_0)/l_0$ due to relaxation of GeS_2 glass at 462 °C.

length contraction $\Delta = (l - l_0)/l_0$ on the logarithmic time scale. It is seen that during the experimental time scale (t_{exp} = 10 h, contraction: 4.15 μm), it is not possible to attain metastable equilibrium. The equilibrium state can be estimated assuming linear extrapolation of supercooled liquid: $\Delta_\infty = \Delta\alpha \cdot (T - T_g^{dil})$, where $\Delta\alpha = \alpha_l - \alpha_g$. The inflectional tangent intersects the ordinates at zero and Δ_∞ corresponding to time t_0 and t_m, respectively. The estimated stabilization period of structural relaxation for GeS_2 glass, isothermally annealed at 462 °C, is $\log(t_m/t_0) = 2.38$. This value is just double than that for the exponential relaxation (1.18).[31]

During the isothermal annealing the glassy structure becomes gradually more and more compact, which slows down the relaxation process. This self-delaying process involving cooperative movement at a molecular level could be explained by implicit dependence of relaxation time upon the continuously changing structure of glass (nonlinearity), usually described as the partition of the activation energy between a temperature and a structure-dependent term.[32]

Another important aspect of the relaxation is a distribution of relaxation times.[25−27] Both these features lead to a nonexponential relaxation function. As a consequence, the structural relaxation at 462 °C lasts significantly longer ($t_m \cong$ 19 h) than it would be expected by a simple Maxwell model ($\tau_R \approx 63$ s), i.e., without cooperative rearrangements on a molecular scale.

The time evolution of the structural relaxation response is comparable to the experimental time scale for isothermal crystal growth measurement. The estimated volumetric change due to the relaxation process is below 0.5%. It seems that slow structural relaxation in germanium disulfide glass does not affect substantially the crystal growth process, at least 20 K below T_g^{dil}. Therefore, the crystal growth morphology reflects the frozen-in structure of the glassy state involving both α-GeS_2 and β-GeS_2 polymorphs. Isothermal crystal growth experiments reveal that the growth kinetics in the bulk glass is very similar in both cases. However, there are significant differences at the surface and thin film described in the next section.

4.2. Isothermal Crystal Growth Kinetics. The probability that the newly formed crystalline phase is retained within the amorphous phase or in the supercooled liquid phase is usually expressed as $[1 - \exp(-\Delta G/RT)]$, where ΔG is the Gibbs energy difference between the vitreous phase or supercooled liquid and the crystalline phase. By definition ΔG is given by

$$\Delta G = \Delta H - T \times \Delta S \quad (3)$$

This can be expanded by using the well-known expression for ΔH and ΔS, considering the heat capacity difference between the two phases $\Delta C_p = C_p^{m} - C_p^{cr}$:

$$\Delta G = \Delta H_m \frac{\Delta T}{T_m} - \int_T^{T_m} \Delta C_p dT + T \int_T^{T_m} \Delta C_p \frac{dT}{T} \quad (4)$$

where ΔH_m is the enthalpy of melting of the pure crystalline substance, T_m is the melting temperature and ΔT is supercooling ($\Delta T = T_m - T$).

Figure 5 shows the temperature dependence of molar heat capacity of germanium disulfide glass[17] and crystalline α-GeS_2.[33] The heat capacity of supercooled liquid of the same

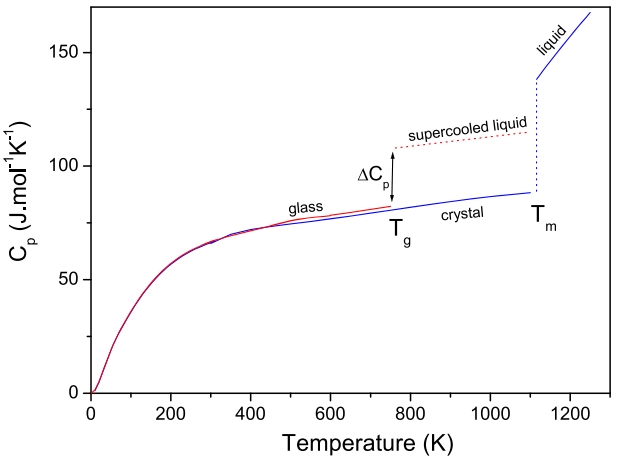

Figure 5. Temperature dependence of molar heat capacity of crystalline α-GeS_2 and germanium disulfide glass and liquid.[17,33]

https://doi.org/10.1021/acs.jpcb.1c03243
J. Phys. Chem. B XXXX, XXX, XXX−XXX

composition is nearly constant and it can be estimated from DSC measurements in the glass transition range.[23] In this case, eq 4 can be simplified as follows:

$$\Delta G = \Delta S_m \Delta T + \Delta C_p[T\ln(T_m/T) - \Delta T] \quad (5)$$

The Gibbs energy difference between the crystalline and vitreous phase or the supercooled liquid phase can easily be calculated by eq 4 as a function of supercooling, assuming $\Delta S_m = \Delta H_m/T_m = 20.61$ J K^{-1} mol^{-1}, $\Delta C_p = 24.6$ J K^{-1} mol^{-1}, and $T_m = 1116$ K.[23,33] The calculated $\Delta G(\Delta T)$ dependence is compared with some approximations in Figure 6. It is evident

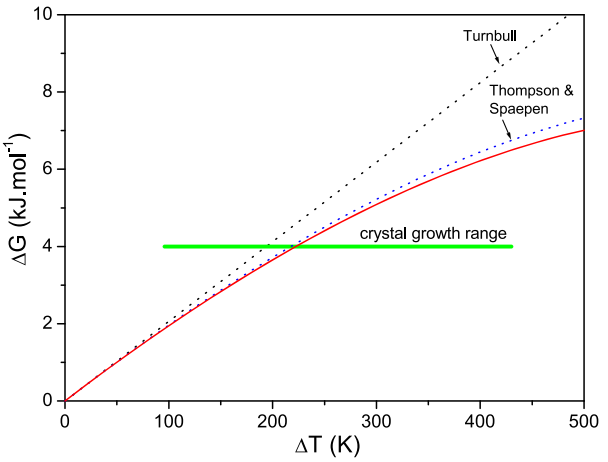

Figure 6. Gibbs energy difference between supercooled liquid and crystalline GeS_2. Broken lines correspond to the Turnbull and Thompson-Spaepen[34] approximation and the full line to calculation by eq 5.

that the Turnbull approximation ($\Delta G \cong \Delta S_m \Delta T$) overestimates ΔG nearly by 40% at the highest supercoolings. On the other hand, Thompson-Spaepen[34] approximation provides much better results (~4%).

The crystal growth rate u obtained by microscopy measurement can be related to the molecular growth rate u_{kin} at the crystal−liquid/amorphous phase interface by the following equation:

$$u_{kin} = \frac{u}{1 - \exp(-\Delta G/RT)} \quad (6)$$

The molecular growth rate is proportional to self-diffusion. However, the temperature dependence of the self-diffusion coefficient is not always available, usually being replaced by the inverse shear viscosity η^{-1} according to the Stokes-Einstein equation.

For the growth processes taking place at the crystal−liquid/amorphous phase interface, we can use the method proposed by Jackson, Uhlmann, and Hunt[35] that is based on inspection of the plot of the reduced growth rate U_R versus supercooling ΔT, defined as:

$$U_R = u_{kin}\eta \quad (7)$$

The temperature dependence of viscosity of GeS_2 supercooled liquid can be expressed by eq 2. The $U_R(\Delta T)$ plot provides an information about the fraction of preferred sites at the interface of the growing crystal. For two-dimensional surface growth (2Dsg), we should expect a nonlinear curve with an increasing positive slope. The $U_R(\Delta T)$ plot for crystal growth in the bulk and at the surface of germanium disulfide glass is shown in Figure 7. Both dependences suggest the 2Dsg growth. In this case, the crystal growth velocity can be described by a two parameter model as[35,36]

$$u = \frac{C}{\eta}\exp\left(\frac{B}{T\Delta T}\right) \quad (8)$$

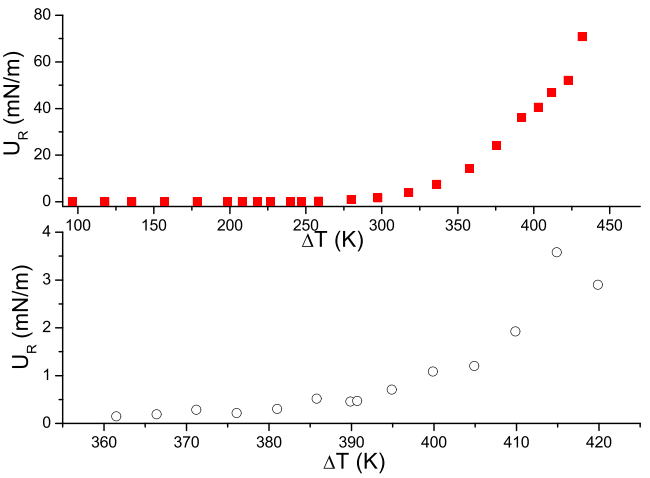

Figure 7. Reduced crystal growth dependence on supercooling for bulk (upper part) and surface (lower part) in germanium disulfide glass.

According to eq 8, the ln $(\eta \cdot u)$ vs $1/T\Delta T$ plot should be a straight line with a negative slope equal to B and the intercept is ln C. Figure 8 shows this plot for all data summarized in

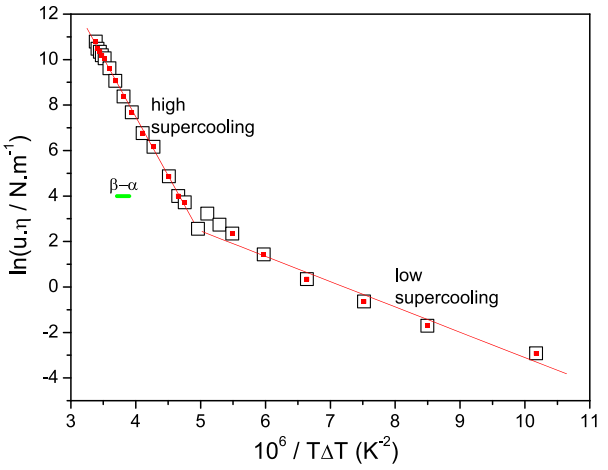

Figure 8. Plot of logarithm (growth velocity × viscosity) versus $1/T\Delta T$ for crystal growth in the bulk of germanium disulfide glass. The solid lines correspond to the least square fit for high and low supercooling.

Table 2. In fact, there are two distinct regions with different parameters. The following parameters were found for high supercooling ln(C/N m^{-1}) = 28.2 ± 0.2, B = (5.18 ± 0.06) × 10^6 K^2 and low supercooling ln(C/N m^{-1}) = 8.0 ± 0.7, B = (1.11 ± 0.10) × 10^6 K^2.

Figure 9 shows experimental values of crystal growth velocity in the bulk of GeS_2 glass and supercooled liquid of the same composition (Table 2) along with the theoretical prediction for the 2Dsg model calculated by eq 8 for B and C parameters corresponding to high and low supercooling. The

https://doi.org/10.1021/acs.jpcb.1c03243
J. Phys. Chem. B XXXX, XXX, XXX−XXX

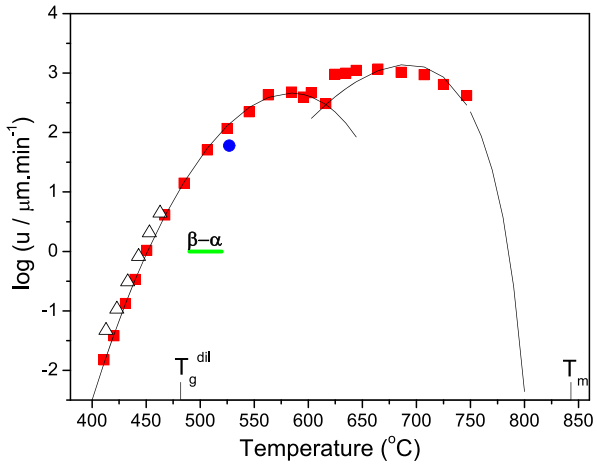

Figure 9. Temperature dependence of crystal growth velocity in germanium disulfide bulk glass and supercooled liquid, Table 2 (red square), the crystal growth of α-GeS_2 thin hexagonal plates below T_g^{dil}, Table 3 (triangle), and previously reported data (blue circle).[37] Solid lines were calculated by eq 8.

high supercooling model well describes bulk crystal growth of β-GeS_2 below T_g^{dil}, mixed growth around $\beta \rightarrow \alpha$ transition, and growth of α-GeS_2 at temperatures up to 510 °C. A slightly higher growth rate following the same model is observed for crystal growth of α-GeS_2 thin hexagonal plates, preexisting in the germanium disulfide glass bulk (Table 3). Voigt and Wolf reported an estimation of crystal growth velocity of spherical aggregates of α-GeS_2 (Kristallkugeln).[37] Their isothermal measurement (~1 μm·s^{-1} at 800 K) is in reasonable agreement with our data (Figure 9). The low supercooling model describes α-GeS_2 growth at higher temperatures above 520 °C.

Figure 10 shows the crystal growth velocity of spherulitic β-GeS_2 at the surface of GeS_2 glass (Table 1) and $u(T)$

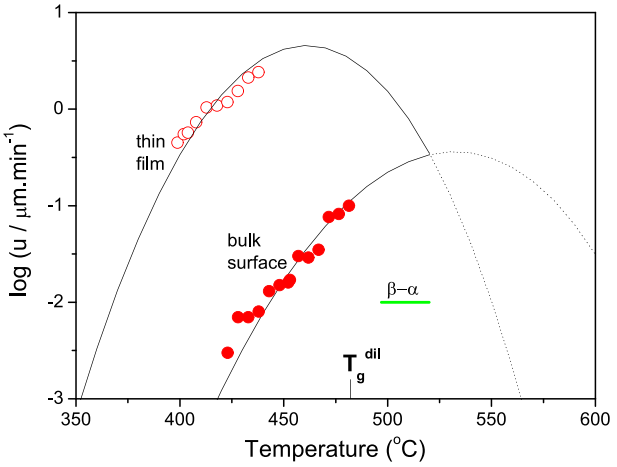

Figure 10. Temperature dependence of crystal growth velocity of β-GeS_2 (red solid circle) at the GeS_2 glass surface and thin film of the same composition (red open circle).[38] Solid and broken lines were calculated by eq 8.

dependences calculated by eq 8 for the parameters: ln(C/N m^{-1}) = 40.5 ± 1.3 and $B = (9.8 \pm 0.4) \times 10^6$ K^2. Previously reported data and $u(T)$ plots for the same growth morphology in germanium disulfide thin films[38] are shown for comparison.

The parameter B in eq 8 can be expressed as[35]

$$B = \pi\lambda V_m \sigma_E^2 / 3k_B \Delta S_m \quad (9)$$

where λ is the molecular diameter and V_m is the molar volume. σ_E is the interface energy of the growing nucleus. Assuming from the crystal data[4] that $V_m = 4.7 \times 10^{-5}$ m^{3}mol^{-1} and $\lambda = (6V_{cell}/\pi Z)^{1/3} = 5.3 \times 10^{-10}$ m, and from the thermodynamic data[33] that $\Delta S_m = 20.61$ J mol K^{-1} we can estimate by eq 9 the nucleus interface energy $\sigma_E \cong 0.11$ J m^{-2} for crystal growth of β-GeS_2 at low supercooling and α-GeS_2 at high supercooling ($\sigma_E \cong 0.24$ J m^{-2}). An even higher value ($\sigma_E \cong 0.33$ J m^{-2}) was found for β-GeS_2 crystal growth at the bulk surface.

There are several significant points revealed by the data in Figures 9 and 10. First, a measurable crystal growth in the bulk, at the bulk surface, and the amorphous thin film takes place below T_g^{dil}. Second, the spherulitic crystallization of the β-GeS_2 phase in the amorphous thin film grows significantly faster than spherulites at the bulk surface ($u_{TF}/u_B \cong 400$). The fast surface crystal growth in the thin film is combined with a weaker viscosity dependence. Similar behavior is well known for many molecular materials.[39] Third, the velocity of α-GeS_2 spherical aggregates growing above T_g^{dil} agrees with previously reported data and follows the prediction for spherulitic crystal growth of β-GeS_2 in bulk glass. However, it is less temperature-dependent at higher temperatures (low supercooling) and, therefore, different 2Dsg models have to be used, accounting for double increase of the interface energy. The intersection point of both 2Dsg model functions is around 616 °C where secondary nucleation is observed.

Simultaneous crystallization of the α-GeS_2 and β-GeS_2 phase in the bulk sample with preexisting α-GeS_2 crystals takes place about 70 K below T_g (Figure 9). It was also shown that α-GeS_2 spherulite grown at temperatures near the maximum growth rate (~700 °C) is gradually transformed to characteristic white crystals of β-GeS_2 after annealing below T_g (central and external part of spherulites, Figure 1a). This probably indicates that there are similar motifs resembling these crystalline polymorphs in the amorphous structure and that both the 2D layer network and the 3D random network are plausible descriptions reproducing experimental data of GeS_2 glass as suggested by Itoh.[19] Recent precise measurement of X-ray diffraction on $Ge_{33}S_{67}$ glass clearly indicates that the first neighboring atomic pair is only a Ge−S bond in this glass. The calculated coordination numbers for Ge and S are 3.77 ± 0.08 and 1.86 ± 0.04, respectively.[40] The relatively low value of Poisson's ratio (υ = 0.28)[29] for GeS_2 glass indicates an intermediate between the highly cross-linked 3D network and the weakly correlated 2D network.[41,42] This is likely also the reason why it is so difficult to prepare pure crystalline β-GeS_2 by crystallization of a glass precursor by a thermal treatment. It seems that the final product is always contaminated by the α-GeS_2 phase, even when the treatment takes place well below the $\beta \rightarrow \alpha$ transition range, except the glassy precursor, which has been carefully purified by distillation.[21,37] Therefore, for synthesis of high purity β-GeS_2, the high-pressure hydrothermal synthesis described by Wang and Horn[5] or the hydrogen sulfide synthesis described by Sutherland et al.[43,44] should be considered.

Significantly higher crystal growth velocity of β-GeS_2 in the amorphous thin film vs bulk surface connected with weaker viscous flow dependence clearly indicates that the molecular crystal growth rate and viscosity are probably decoupled; this is discussed further, below.

https://doi.org/10.1021/acs.jpcb.1c03243
J. Phys. Chem. B XXXX, XXX, XXX−XXX

4.3. Crystal Growth Decoupling from Viscosity. It was mentioned earlier that the molecular growth rate u_{kin} is expected to be proportional to diffusivity D and inversely proportional to the shear viscosity η^{-1}. However, Ediger et al.[45] reported the crystal growth velocity decoupling from viscosity for a wide range of organic and inorganic materials:

$$u_{kin} \propto \eta^{-\xi} \tag{10}$$

where the exponent ξ is smaller than unity. On the basis of these data, it was assumed[45] that the exponent ξ depends on fragility of supercooled liquid m near the glass transition ($\xi \cong 1.1-0.005$ m). Fragility of GeS_2 is between the strong and fragile limits ($m \cong 35.3$).[29] Therefore, the kinetic exponent is estimated as $\xi \cong 0.92$. This would indicate only a slight decoupling between crystal growth and viscosity temperature dependences. In fact, the crystallization kinetics is more complex in the GeS_2 glass.

Figure 11 shows the u_{kin} vs viscosity plot in a log−log format calculated by eqs 2, 5, and 6 from temperature-dependent

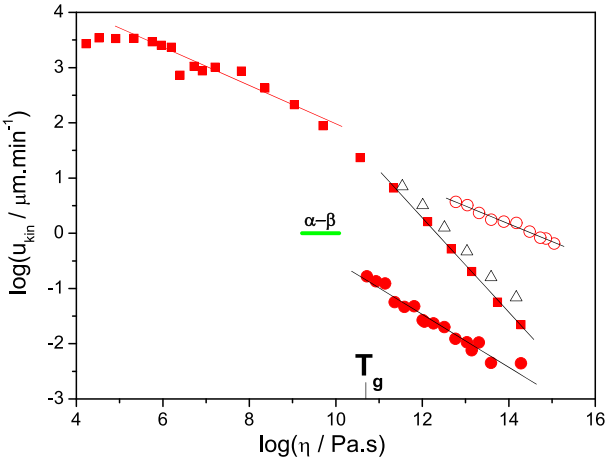

Figure 11. Viscosity scaling of crystal growth velocity in germanium disulfide bulk glass and supercooled liquid (red solid square), the growth of α-GeS_2 thin hexagonal plates in the bulk glass (triangle), the growth of β-GeS_2 at the GeS_2 glass surface (red solid circle), and the thin film of the same composition (red open circle).[38] Solid lines correspond to the least square fit of eq 10.

crystal growth velocity data (Tables 123) and the Gibbs energy difference between supercooled liquid/glassy and crystalline GeS_2. The slope of the solid line corresponding to the least square fit of eq 10 is equal to the exponent ξ for the bulk material. Its value for crystal growth of β-GeS_2 in the bulk glass at large supercooling is $\xi = 0.86 \pm 0.02$. A very similar value is found for the crystal growth of preexisting α-GeS_2 in the same temperature range. However, a significantly smaller value ($\xi = 0.35 \pm 0.02$), indicating substantial decoupling between crystal growth and viscosity, is found for crystal growth of α-GeS_2 at lower supercooling. A comparable value was found for spherulitic crystal growth of β-GeS_2 in amorphous germanium disulfide thin films ($\xi = 0.32 \pm 0.02$) and at the bulk glass surface ($\xi = 0.48 \pm 0.03$).

A similar contrasting behavior between the bulk, surface, and thin film was recently reported for the spherulitic crystal growth kinetics in amorphous selenium (a-Se). Only slight decoupling was observed for slower crystal growth in bulk a-Se at large supercooling ($\xi = 0.94$).[46] Significantly more pronounced decoupling was found for faster crystal growth at the surface of a-Se and selenium thin films ($\xi = 0.67$).[47] The spherulitic crystallization in the amorphous selenium thin film is about two orders of magnitude faster than that in a-Se bulk glass.[47]

Such behavior resembles the "diffusionless" GC (glass-to-crystal) fast growth mode observed in some molecular organic glass formers such as *o*-terphenyl, reported by many authors and nicely summarized and discussed by Xi et al.[48] This GC mode in *o*-terphenyl is activated above T_g as loose, fast-growing fibers and continues deep in the glassy state yielding in compact spherulites. This growth mode is remarkable because upon its activation the relation $u_{kin} \propto D$ breaks down, justifying the description "diffusionless".[48] Similarly, the crystal growth decoupling from viscosity for *o*-terphenyl is significant. Taking into account all data for the GC growth mode, summarized by Xi et al.[48] we can find $\xi = 0.20$. In contrast, a standard growth mode in supercooled liquid of *o*-terphenyl provides a considerably higher value $\xi = 0.76$.[45] The velocity of crystal growth as well as the diffusivity can be even faster (up to 8 orders of magnitude) at the free surface of molecular glass.[49−51] It has been shown by Huang et al.[39] for many molecular glasses that the surface crystal growth rate u_s is roughly proportional to the surface diffusion coefficient D_s, regardless the molecular details ($u_s \propto D_s^{0.87}$). Recently, it was reported that surface mobility in amorphous selenium scales in the same way as the surface crystal growth rate.[52]

It is interesting to compare the density of germanium disulfide bulk glass (2.72 g cm^{-3})[30,53] α-GeS_2 (2.89 g cm^{-3})[3] and β-GeS_2 (2.99 g cm^{-3}).[2] The crystallization of glassy material, therefore, causes increase in density by 6.3% for the high temperature α polymorph and 9.9% for the low temperature β polymorph. An even larger increase can be expected for a thin film. Such density increase is considerably higher than values reported for typical molecular glasses,[39] which suggests that there are voids, cracks, and new surfaces created due to crystal growth in glassy material. With respect to these substantial volumetric changes, estimated contraction due to the structural relaxation process is negligible (< 0.5%).

Schmelzer et al.[54] suggested that the growth of higher density crystals in the glassy matrix of lower density creates an elastic strain causing slower crystallization rates in the bulk. Other authors argued that the tension around a crystal growing in glassy material should increase the crystal growth rate in the bulk.[55] These two models provide contradictory predictions for surface crystal growth. Gunn et al.[56] tested both models for crystal growth of carbamazepine, concluding that the crystal density has no controlling effect on the difference between surface and crystal growth rates. A better explanation of fast GC growth below the glass transition is based on the possible role of fracture and surface mobility.[57]

The decoupling parameter ξ can also be estimated from activation energy of crystal growth and viscosity as described in the next section.

4.4. Activation Energy of Crystal Growth. In a relatively narrow temperature range, the isothermal crystal growth velocity of α-GeS_2 and β-GeS_2 polymorphs can be described by Arrhenius temperature dependence. The activation energy of crystal growth E_G then corresponds to the slope of such dependence in the logarithmic scale:

$$\frac{d\log(u)}{d(1/T)} = \frac{-E_G}{R\cdot\ln(10)} \tag{11}$$

https://doi.org/10.1021/acs.jpcb.1c03243
J. Phys. Chem. B XXXX, XXX, XXX−XXX

Figure 12 shows the experimental crystal growth data in the bulk glass and supercooled liquid (Table 2). The activation

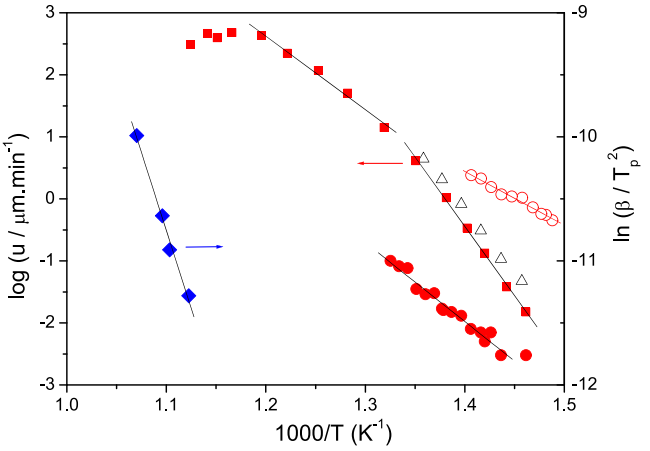

Figure 12. Determination of the activation energy of β-GeS_2 crystal growth in the bulk glass (red solid square), the bulk surface (red solid circle), and the thin film (red open circle). The estimation of apparent activation energy by the Kissinger method[62] (eq 15) is shown for a comparison (blue solid diamond). Solid lines correspond to least square fits to experimental data.

energy of β-GeS_2 growth at the surface of the glassy sample is E_G = 244 ± 13 and 166 ± 8 kJ mol^{-1} in the thin film.[38] The $\log(u)$ vs $1/T$ dependence for crystal growth is more complex in a broader temperature range. While the activation energy of β-GeS_2 growth at large supercooling is E_G = 427 ± 9 kJ mol^{-1}, a considerably lower value is found for α-GeS_2 growth at lower supercooling (E_G = 196 ± 20 kJ mol^{-1}). Within combined error limits, this value is comparable to the apparent activation energy found from DSC experiments.

The exponential term in eq 6 can be neglected for moderate entropy of melting ($\Delta S_m/R$ = 2.47) and supercooling $\Delta T >$ 300 K. The decoupling parameter ξ then can be expressed as[58]

$$\xi \cong E_G/E_\eta \tag{12}$$

where E_η is the activation energy of viscous flow, estimated as E_η = 462 kJ/mol.[28] The decoupling parameter calculated from eq 12 is ξ = 0.92 for β-GeS_2 crystal growth in the bulk, ξ = 0.53 at the glassy surface, and ξ = 0.36 in the thin film. These values are consistent with the ξ found from log u vs log η plots.

Activation energies are relevant for any time scales being inherently dependent in choosing an appropriate temperature range. Their physical interpretation is more challenging in such cases for which a reaction barrier is not readily identifiable.[59] This is important for nonisothermal crystallization kinetics where a complex nucleation and growth phenomena are studied indirectly by heat flow evolved during DSC constant heating rate experiments.

4.5. Nonisothermal Crystallization Kinetics. The crystallization data were obtained at different heating rates by means of DSC. Usually, it is assumed that the rate of the crystallization process is proportional to the measured heat flow, ϕ, normalized per sample mass. It is also assumed that the temperature dependence of the rate constant follows an Arrhenius form. The heat flow due to crystallization then can be expressed as[60,61]

$$\phi = \Delta H_c A \exp(-E/RT)\cdot f(\alpha) \tag{13}$$

where A is the preexponential factor and E is the apparent activation energy describing a complex crystallization process. The function $f(\alpha)$ represents the kinetic model of the crystallization process. The fraction crystallized, α, can be obtained by a partial integration of $\phi(T)$ dependence after baseline subtraction:[60,61]

$$\alpha = \frac{1}{\Delta H \beta}\int_{T_{onset}}^{T} \phi \cdot dT \tag{14}$$

where T_{onset} corresponds to the beginning of the baseline approximation and β is the heating rate. The validity of eqs 13 and 14 should always be verified.[60]

Figure 13 shows the kinetic data extracted from the DSC crystallization peak illustrated in Figure 2 (points). These data

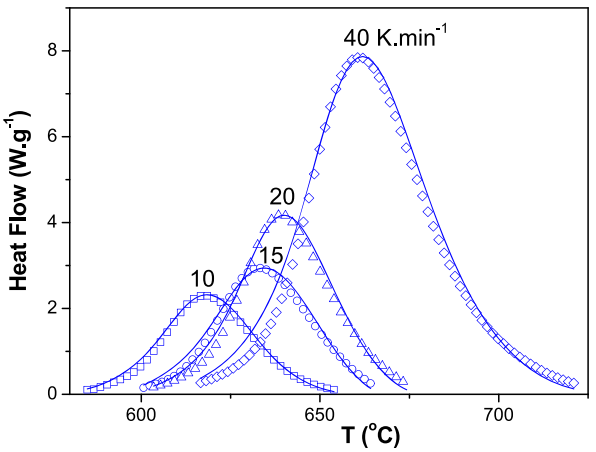

Figure 13. Experimental DSC crystallization curves of $Ge_{33}S_{67}$ glass for different heating rates β (points). Solid lines were calculated by eqs 11 and 17 for the parameters: ln (A/s^{-1}) = 24.2 ± 0.1, E = 209 ± 13 kJ mol^{-1}, M = 0.55 ± 0.05, and N = 1.1 ± 0.1.

reflect the whole crystallization process, possibly involving surface as well as the bulk crystal growth. Any direct comparison of experimental $\phi(T)$ dependences is complicated by the fact that they depend on α, β, and T. Moreover, the kinetic parameters A and E are strongly correlated. For this reason, the nonlinear regression cannot be recommended for the kinetic analysis of $\phi(T)$ data unless the parameter E is known. Therefore, the determination of the activation energy should be a first step of any kinetic analysis of nonisothermal data.

The apparent activation energy characterizing the non-isothermal crystallization process can be determined by the Kissinger method[62] from the temperature shift of the maximum of DSC peak T_p with the heating rate:

$$\frac{d\ln(\beta/T_p^2)}{d(1/T_p)} = \frac{-E}{R} \tag{15}$$

The typical Kissinger plot is shown in Figure 12. The apparent activation energy determined from the slope of this plot using eq 15 is E = 209 ± 13 kJ mol^{-1}. This value is not so different from the values previously reported by Voigt and Ludwig[63] (219 ± 15 kJ mol^{-1}) and other authors[64] (210 ± 7 kJ mol^{-1}).

The kinetic model of the crystallization process $f(\alpha)$ in eq 13 should be invariant with respect to A, E, and β. It can be

https://doi.org/10.1021/acs.jpcb.1c03243
J. Phys. Chem. B XXXX, XXX, XXX−XXX

shown[60,65] that similar behavior can be expected also for the functions $y(\alpha)$ and $z(\alpha)$ defined as

$$y(\alpha) = \phi(T)\cdot\exp(E/RT) \propto f(\alpha) \tag{16a}$$

$$z(\alpha) = \phi(T)\cdot T^2 \propto f(\alpha)\int_0^a \frac{d\alpha}{f(a)} \tag{16b}$$

Therefore, the function $y(\alpha)$ is obtained by multiplying the measured heat flow by the exponential term $\exp(E/RT)$ and it should be proportional to the kinetic model $f(\alpha)$. $z(\alpha)$ is easily obtained by multiplying the measured heat flow by the square of temperature.[60]

Figure 14 shows these functions converted by eqs 16a and 16b from the experimental DSC data (Figure 13). For easier

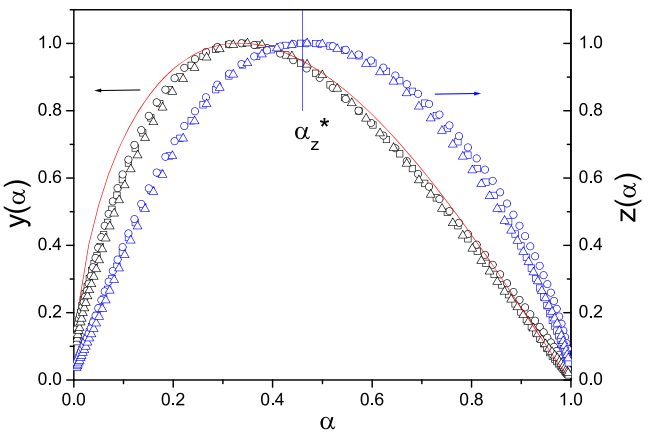

Figure 14. $y(\alpha)$ and $z(\alpha)$ functions obtained by transformation of DSC data shown in Figure 13. Points were calculated by eqs 16a and 16b (identical symbols). The solid line was calculated by eq 17 for M = 0.55 and N = 1.1.

comparison of data sets for different heating rates, the functions are normalized within (0,1) range. There are three conclusions that can be drawn from this figure. First, for each function, all data corresponding to different heating rates collapse on a single curve. This clearly indicates that eq 11 can be used for a quantitative description of experimental data. Second, the maximum of the $z(\alpha)$ function (α_z^* = 0.46 ± 0.02) is considerably lower than it could be expected for a standard Johnson-Mehl-Avrami (JMA) nucleation-growth model (0.632).[60,65]

The JMA model was originally derived for isothermal conditions and later extended to nonisothermal conditions under certain assumptions.[66,67] It seems that these assumptions are not fulfilled for the crystallization in GeS_2 glass. Third, the shape and maximum α_y^* = 0.33 ± 0.03 of the $y(\alpha)$ function indicate that the autocatalytic model can be used in this case:

$$f(\alpha) = \alpha^M(1-\alpha)^N \tag{17}$$

The kinetic exponents M = 0.55 ± 0.05 and N = 1.1 ± 0.1 can be calculated by the method described elsewhere.[68] This function is plotted by a solid line in Figure 14. The autocatalytic model reflects the self-accelerating nature of fast crystal growth where relatively large crystallization heat is generated during the DSC experiment (ΔH_c = − 102 J/g). The model fits the data quite well except for α < 0.2 where it slightly overestimates experimental results. Knowing the value of apparent activation energy E = 209 ± 13 kJ mol^{-1}, ln (A/s^{-1}) = 24.2 ± 0.1, and the kinetic model defined by eq 17, the DSC curves can be calculated by eq 13. These curves (solid lines) are compared with the experimental data in Figure 13.

The apparent activation energy characterizing the nonisothermal crystallization process monitored by DSC is close to the activation energy of microscopic crystal growth found in a comparable temperature range (E_G = 196 ± 20 kJ mol^{-1}). It seems, therefore, that the Arrhenius type kinetic equation (eq 13) is justified in this case and the apparent activation energy found by the Kissinger method from nonisothermal DSC data might be associated entirely with the crystal growth kinetics of α-GeS_2. This indicates that despite the complex nature of nonisothermal kinetics captured by DSC experiments, the crystal growth is likely the rate-controlling step in overall crystallization of GeS_2 glass. A similar conclusion was drawn from calorimetric and microscopic crystal growth data in selenium[46] and As_2Se_3 supercooled liquid.[58] On the other hand, the parameters M and N indicate a relatively fast increase in the initial crystallization rate that might be due to a secondary nucleation induced by crystal growth.[61,69] This, in combination with impingement of growing crystals, can be a plausible explanation why the standard JMA model cannot be used for the description of nonisothermal calorimetric data. Nevertheless, for a more detailed assessment of nanoscale dynamics at the crystal-melt interface, X-ray photon correlation spectroscopy seems to be promissing.[70]

5. CONCLUSIONS

In this article, we extended the previously reported crystal growth in GeS_2 thin films[38] by a detailed study of the isothermal crystal growth kinetics and morphology in germanium disulfide bulk glass and glass surface, involving low temperature β-GeS_2 and high temperature α-GeS_2 polymorphs. The time evolution of the structural relaxation is comparable to the experimental time scale for these isothermal crystal growth measurements. It seems that slow structural relaxation does not affect substantially the crystal growth process, below the glass transition in germanium disulfide glass. The crystal growth in the bulk glass is only slightly decoupled from shear viscosity (ξ = 0.86). It is also faster than spherulitic crystal growth of the β-GeS_2 phase at the surface of the bulk glass. However, the crystal growth of β-GeS_2 in amorphous thin films of the same composition is several orders of magnitude faster than that at the surface of bulk glass. The surface crystal growth in the bulk glass and thin film is weakly dependent on viscosity (ξ = 0.32). Such behavior resembles the "diffusionless" GC (glass-to-crystal) fast growth mode observed in some molecular organic glass formers such as *o*-terphenyl, tris-naphtylbenzene, indomethacin, and nifedipine, reported by several authors.

Taking into account previously reported viscosity[28] and heat capacity data,[17,33] the crystal growth kinetics of both polymorphs can be quantitatively described by the surface growth model (2Dsg) for the nucleus interface energy $\sigma_E \cong$ 0.11 J m^{-2} at low supercooling and $\sigma_E \cong$ 0.24 J m^{-2} at high supercooling. The activation energy of crystal growth obtained from microscopy experiments at low supercooling (E_G = 196 ± 20 kJ mol^{-1}) is comparable within combined error limits to the apparent activation energy found from DSC experiments in the same temperature range (E = 209 ± 13 kJ mol^{-1}). This indicates that the crystal growth is probably the rate-controlling step in nonisothermal crystallization kinetics in GeS_2 glass.

https://doi.org/10.1021/acs.jpcb.1c03243
J. Phys. Chem. B XXXX, XXX, XXX−XXX

AUTHOR INFORMATION

Corresponding Author

Jiří Málek − *Department of Physical Chemistry, Faculty of Chemical Technology, University of Pardubice, Pardubice 532 10, Czech Republic;* orcid.org/0000-0002-7502-5320; Email: jiri.malek@upce.cz

Authors

Veronika Podzemná − *Department of Physical Chemistry, Faculty of Chemical Technology, University of Pardubice, Pardubice 532 10, Czech Republic*

Jana Shánělová − *Department of Physical Chemistry, Faculty of Chemical Technology, University of Pardubice, Pardubice 532 10, Czech Republic;* orcid.org/0000-0001-5517-7434

Complete contact information is available at: https://pubs.acs.org/10.1021/acs.jpcb.1c03243

Notes

The authors declare no competing financial interest.

ACKNOWLEDGMENTS

This work was partially supported by the project CZ1.07/2.3.00/20.0254 "ReAdMat - Research Team for Advanced Non-Crystalline Materials" (European Social Fund and Ministry of Education, Youth and Sports, Czech Republic) and the Selected Research Teams program of University of Pardubice.

REFERENCES

(1) Yang, Y.; Liu, S. C.; Wang, X.; Li, Z.; Zhang, Y.; Zhang, G.; Xue, D. J.; Hu, J. S. Polarization-Sensitive Ultraviolet Photodetection of Anisotropic 2D GeS_2. *Adv. Funct. Mater.* **2019**, *29*, No. 1900411.

(2) Wang, X.; Tan, J.; Han, C.; Wang, J. J.; Lu, L.; Du, H.; Jia, C. L.; Deringer, V. L.; Zhou, J.; Zhang, W. Sub-Angstrom Characterization of the Structural Origin for High In-Plane Anisotropy in 2D GeS_2. *ACS Nano* **2020**, *14*, 4456−4462.

(3) Dittmar, G.; Schäffer, H. Die Kristallstruktur von H.T.-GeS_2. *Acta Crystallogr.* **1975**, *B31*, 2060−2064.

(4) Dittmar, G.; Schäffer, H. Die Kristallstruktur von L.T.-GeS_2. *Acta Crystallogr.* **1976**, *32*, 1188−1192.

(5) Wang, N.; Horn, E. E. β-GeS_2 synthesis and crystal data. *N. Jb. Miner. Mh.* **1975**, 41−44.

(6) Viaene, W.; Moh, G. H. The Condensed Germanium-Sulfur System. *N. Jb. Miner. Mh.* **1970**, 283−285.

(7) Wang, Q.; Kang, S. Z.; Li, X.; Yang, Y. W.; Qin, L.; Mu, J. A facile preparation of crystalline GeS_2 nanoplates and their photocatalytic activity. *J. Alloys Compd.* **2015**, *631*, 21−25.

(8) Armand, P.; Ibanez, A.; Dexpert, H.; Philippot, E. Short and medium range order in germanium sulfide glasses: a low-temperature X-ray absorption spectroscopy study. *J. Non Cryst. Solids* **1992**, *139*, 137−145.

(9) Petri, I.; Salmon, J. A neutron diffraction study of glassy GeS_2. *J. Non Cryst. Solids* **2001**, *293-295*, 169−174.

(10) Bychkov, E.; Miloshova, D. I.; Price, C. J.; Benmore, A.; Lorriaux, A. Short, intermediate and mesoscopic range order in sulfur-rich binary glasses. *J. Non Cryst. Solids* **2006**, *352*, 63−70.

(11) Blaineau, S.; Jund, P. Vibrational signature of broken chemical order in a GeS_2 glass: A molecular dynamics simulation. *Phys. Ther. Rev.* **2004**, *69*, No. 064201.

(12) Celino, M.; Le Roux, S.; Ori, G.; Coasne, B.; Bouzid, A.; Boero, M.; Massobrio, C. First-principles molecular dynamics study of glassy GeS_2: Atomic structure and bonding properties. *Phys. Rev. B* **2013**, *88*, No. 174201.

(13) Phillips, J. C. Topology of covalent non-crystalline solids II: Medium-range order in chalcogenide alloys and a-Si(Ge). *J. Non Cryst. Solids* **1981**, *43*, 37−77.

(14) Weinstein, B. A.; Zallen, R.; Slade, M. I.; Mikkelsen, J. C., Jr. Pressure-Optical Studies of GeS_2 Glasses and Crystals−Implications for Network Topology. *Phys. Rev. B* **1982**, *25*, 781−792.

(15) Boolchand, P.; Grothaus, J.; Tenhover, M.; Hazle, M. A.; Grasselli, R. K. Structure of GeS_2 glass − Spectroscopic evidence for broken chemical order. *Phys. Rev. B* **1986**, *33*, 5421−5434.

(16) Kawamoto, Y.; Kawashima, C. Infrared and Raman-Spectroscopic Studies on Short-Range Structure of Vitreous GeS_2. *Mater. Res. Bull.* **1982**, *17*, 1511−1516.

(17) Málek, J.; Chovanec, J.; Svoboda, R.; Taniguchi, Y.; Kawaji, H. Heat capacity of vitreous GeS_2. *J. Chem. Thermodyn.* **2015**, *81*, 101−108.

(18) Černošek, Z.; Černošková, E.; Beneš, L. Raman scattering in GeS_2 glass and its crystalline polymorphs compared. *J. Mol. Struct.* **1997**, *435*, 193−198.

(19) Itoh, K. Structural study of GeS_2 glass: Reverse Monte Carlo modelling for edge-sharing tetrahedral network. *J. Phys. Chem. Solid* **2017**, *103*, 109−115.

(20) Málek, J.; Klikorka, J.; Beneš, L.; Tichý, L.; Tříska, A. Electrical amd optical properties of $Ge_{20}Sb_{15-x}Bi_xS_{65}$ glasses. *J. Mater. Sci.* **1986**, *21*, 488−492.

(21) Voigt, B. Über Glasbildung und Eigenschaften von Chalkogenidsystemen, XVII. Zur Glaschemie des Germaniumdisulfides. *Z. anorg. allg. Chem.* **1978**, *447*, 153−160.

(22) Shánělová, J.; Málek, J.; Alcalá, M. D.; Criado, J. M. Kinetics of crystal growth of germanium disulfide in $Ge_{0.38}S_{0.62}$ chalcogenide glass. *J. Non Cryst. Solids* **2005**, *351*, 557−567.

(23) Málek, J. The glass transition and crystallization of germanium-sulphur glasses. *J. Non Cryst. Solids* **1989**, *107*, 323−327.

(24) O'Hare, P. A. G.; Volin, K. J.; Susman, S. Thermochemistry of (germanium+sulfur) III. Massic energies of combustion in fluorine and the derived standard molar enthalpies of formation of crystalline and vitreous germanium (IV) disulfide GeS_2. *J. Chem. Thermodyn.* **1995**, *27*, 99−110.

(25) Angell, C. A.; Ngai, K. L.; McKenna, G. B.; McMillan, P. F.; Martin, S. W. Relaxation in glassforming liquids and amorphous solids. *J. Appl. Phys.* **2000**, *88*, 3113−3157.

(26) Ediger, M. D.; Angell, C. A.; Nagel, S. R. Supercooled Liquids and Glasses. *J. Phys. Chem.* **1996**, *100*, 13200−13212.

(27) Mauro, J. C.; Yue, Y.; Ellison, A. J.; Gupta, P. K.; Allan, D. C. Viscosity of glass-forming liquids. *PNAS* **2009**, *106*, 19780−19784.

(28) Málek, J.; Shánělová, J. Viscosity of germanium sulfide melts. *J. Non Cryst. Solids* **1999**, *243*, 116−122.

(29) Ota, R.; Kunugi, M. Temperature and pressure dependence of the elastic property of GeS_2 glass. *J. Phys. Chem. Solid* **1977**, *38*, 9−13.

(30) Cavagna, A. Supercooled liquids for pedestrians. *Phys. Rep.* **2009**, *476*, 51−124.

(31) Málek, J. Rate-determining factors for structural relaxation in non-crystalline materials I. Stabilization period of isothermal volume relaxation. *Thermochim. Acta* **1998**, 313, 181 − 190; Rate-determining factors for structural relaxation in non-crystalline materials II. Normalized volume and enthalpy relaxation rate. *Thermochim. Acta* **1998**, *313*, 191−200.

(32) Naraynaswamy, O. S. A Model of Structural Relaxation in Glass. *J. Am. Ceram. Soc.* **1971**, 54, 491 - 498; Thermorheological Simplicity in the Glass Transition. *J. Am. Ceram. Soc.* **1988**, *71*, 900−904.

(33) Málek, J.; Mitsuhashi, T.; Ohashi, N.; Taniguchi, Y.; Kawaji, H.; Atake, T. Heat capacity and thermodynamic properties of germanium disulfide at temperatures from T = (2 - 1240 K). *J. Chem. Thermodyn.* **2011**, *43*, 405−409.

(34) Thompson, C. V.; Spaepen, F. On the approximation of the free energy change on crystallization. *Acta Metall.* **1979**, *27*, 1855−1859.

(35) Jackson, K. A.; Uhlmann, D. R.; Hunt, J. On the nature of crystal growth from melt. *J. Cryst. Growth* **1967**, *1*, 1−36.

(36) Kirkpatrick, R. J. Crystal Growth from the Melt: A Review. *Am. Mineral.* **1975**, *60*, 798−814.
(37) Voigt, B.; Wolf, M. Beeinflussung des Kristallisationverhaltens von GeS_2-Schmelzen durch Schwefel oder Arsen. *Monatshefte für Chemie* **1983**, *114*, 1013−1021.
(38) Podzemná, V.; Barták, J.; Málek, J. Crystal growth kinetics in GeS_2 amorphous thin films. *J. Therm. Anal. Calorim.* **2014**, *118*, 775−781.
(39) Huang, C.; Ruan, S.; Cai, T.; Yu, L. Fast Surface Diffusion and Crystallization of Amorphous Griseofulvin. *J. Phys. Chem. B* **2017**, *121*, 9463−9468.
(40) Sakaguchi, Y.; Hanashima, T.; Ohara, K.; Simon, A. A.; Mitkova, M. Structural transformation in Ge_xS_{100-x} ($10 \leq x \leq 40$) network glasses: Structural varieties in short-range, medium-range, and nanoscopic scale. *Phys. Rev. Mater.* **2019**, *3*, 035601−035618.
(41) Rouxel, T. Elastic Properties and Short-to Medium-Range Order in Glasses. *J. Am. Ceram. Soc.* **2007**, *90*, 3019−3039.
(42) Greaves, G. N.; Greer, A. L.; Lakes, R. S.; Rouxel, T. Poisson's ratio and modern materials. *Nat. Mater.* **2011**, *10*, 823−837.
(43) Sutherland, J. T.; Poling, S. A.; Nelson, C. R.; Martin, S. W. H_2S synthesis route for high purity low temperature 3D GeS_2. *J. Mater. Sci. Lett.* **2003**, *22*, 1467−1469.
(44) Sutherland, J. T.; Poling, S. A.; Belin, R. C.; Martin, S. W. Exploration of the Hydrogen Sulfide - Germanium Sulfide System. *Chem. Mater.* **2004**, *16*, 1226−1231.
(45) Ediger, M. D.; Harrowell, P.; Yu, L. Crystal growth kinetics exhibit a fragility-dependent decoupling from vicosity. *J. Chem. Phys.* **2008**, *128*, No. 034709.
(46) Málek, J.; Barták, J.; Shánělová, J. Spherulitic Crystal Growth Velocity in Selenium Supercooled Liquid. *Cryst. Growth Des.* **2016**, *16*, 5811−5821.
(47) Barták, J.; Valdés, D.; Málek, J.; Podzemná, V.; Slang, S.; Pálka, K. Comparison of Lateral Crystal Growth in Selenium Thin Films and Surface of Bulk Samples. *Cryst. Growth Des.* **2018**, *18*, 4103−4110.
(48) Xi, H.; Sun, Y.; Yu, L. Diffusion-controlled ad diffusionless crystal growth in liquid o-terphenyl near its glass transition temperature. *J. Chem. Phys.* **2009**, *130*, No. 094508.
(49) Wu, T.; Yu, L. Surface crystallization of indomethacin below Tg. *Pharm. Res.* **2006**, *23*, 2350−2355.
(50) Musumeci, D.; Hasebe, M.; Yu, L. Crystallization of Organic Glasses: How Does Liquid Flow Damage Surface Crystal Growth? *Cryst. Growth Des.* **2016**, *16*, 2931−2936.
(51) Shi, Q.; Cai, T. Fast Crystal Growth of Amorphous Griseofulvin: Relations between Bulk and Surface Growth Modes. *Cryst. Growth Des.* **2016**, *16*, 3279−3286.
(52) Barták, J.; Málek, J.; Bagchi, K.; Ediger, M. D.; Li, Y.; Yu, L. Surface mobility in amorphous selenium and comparison with organic molecular glasses. *J. Chem. Phys.* **2021**, *154*, No. 074703.
(53) Zhilinskaya, E. A.; Lazukin, V. N. K.; Oblasov, A. K. Ge_xS_{1-x} glasses. Defects, density and structure. *J. Non Cryst. Solids* **1990**, *124*, 48−62.
(54) Schmelzer, J.; Pascova, R.; Müller, J.; Gutzov, I. Surface-induced devitrification of glasses: the influence of elastic strains. *J. Non Cryst. Solids* **1993**, *162*, 26−39.
(55) Konishi, T.; Tanaka, H. Possible origin of enhanced crystal growth in glass. *Phys. Rev. B* **2007**, *76*, 220201−220204.
(56) Gunn, E. M.; Guzei, I. A.; Yu, L. Does Crystal Density Control Fast Surface Crystal Growth in Glasses? A Study with Polymorphs. *Cryst. Growth Des.* **2011**, *11*, 3979−3984.
(57) Powell, T.; Xi, H.; Sun, Y.; Gunn, E.; Chen, Y.; Ediger, M. D.; Yu, L. Fast Crystal Growth in o-Terphenyl Glasses: A Possible Role for Fracture and Surface Mobility. *J. Phys. Chem. B* **2015**, *119*, 10124−10130.
(58) Málek, J.; Shánělová, J.; Martinková, S.; Pilný, P.; Koštál, P. Crystal Growth Velocity in As_2Se_3 Supercooled Liquid. *Cryst. Growth Des.* **2017**, *17*, 4990−4999.
(59) Piskulich, Z. A.; Mesele, O. O.; Thompson, W. H. Activation Energies and Beyond. *J. Phys. Chem. A* **2019**, *123*, 7185−7194.
(60) Málek, J. Kinetic analysis of crystallization processes in amorphopus materials. *Thermochim. Acta* **2000**, *355*, 239−253.
(61) Málek, J.; Mitsuhashi, T.; Criado, J. M. Kinetic analysis of solid-state processes. *J. Mater. Res.* **2001**, *16*, 1862−1871.
(62) Kissinger, H. E. Reaction Kinetics in Differential Thermal Analysis. *Anal. Chem.* **1957**, *29*, 1702−1706.
(63) Voigt, B.; Ludwig, W. Untersuchung der Kristallisation Unterkühlter GeX_2-Schmelzen (X = O, S, Se) durch DTA. *J. Thermal Anal.* **1982**, *25*, 341−346.
(64) Málek, J.; Klikorka, J. Crystallization kinetics of glassy GeS_2. *J. Thermal Anal.* **1987**, *32*, 1883−1893.
(65) Málek, J.; Koga, N.; Pérez-Maqueda, L. A.; Criado, J. M. The Ozawa's generalized time concept and YZ-master plots as a convenient tool for kinetic analysis of complex processes. *J. Therm. Anal. Calorim.* **2013**, *113*, 1437−1446.
(66) Málek, J.; Mitsuhashi, T. Testing Method of the Johnson-Mehl-Avrami Equation in Kinetic Analysis of the Crystallization Processes. *J. Am. Ceram. Soc.* **2000**, *83*, 2103−2105.
(67) Henderson, D. W. Thermal Analysis of Nonisothermal Crystallization Kinetics in Glass Forming Liquids. *J. Non Cryst. Solids* **1979**, *30*, 301−315.
(68) Málek, J. The kinetic analysis of non-isothermal data. *Thermochim. Acta* **1992**, *200*, 257−269.
(69) Málek, J.; Černošková, E.; Švejka, R.; Šesták, J.; Van der Plaats, G. Crystallization kinetics of $Ge_{0.3}Sb_{1.4}S_{2.7}$ glass. *Thermochim. Acta* **1996**, *280-281*, 353−361.
(70) Li, J.; Jangid, R.; Zhu, W.; Kohne, C.; Fluerasu, A.; Zhang, Y.; Sen, S.; Kukreja, R. Dynamics at the crystal-melt interface in a supercooled chalcogenide liquid near the glass transition. *Sci. Rep.* **2020**, *10*, 5881.

https://doi.org/10.1021/acs.jpcb.1c03243
J. Phys. Chem. B XXXX, XXX, XXX−XXX